ARTICLE

Thermochromism of 1,4-Bis[2-(4-pyridyl)ethenyl]-benzene Derivatives

Ning Chu[a], Ai-sen Li[a,b], Shu-ping Xu[a], Wei-qing Xu[a]*

a. State Key Laboratory of Supramolecular Structure and Materials, Institute of Theoretical Chemistry, College of Chemistry, Jilin University, Changchun 130012, China
b. College of Physics, Jilin University, Changchun 130012, China

(Dated: Received on August 1, 2020; Accepted on September 8, 2020)

Three kinds of thermochromic materials (DC8, DC12, DC16) were synthesized by linking the rigid 1,4-bis[2-(4-pyridyl)ethenyl]-benzene (bpeb) with different lengths of alkyl chains. They exhibit remarkable fluorescent color changes under the irradiation of 365 nm light with elevating temperature, which is supposed to be caused by the transition between the crystal state and the amorphous state. Interestingly, the DC16 solid also has a photochromic character. It should be noticed that the phase transition temperatures of three materials measured by differential scanning calorimetry are higher than those of the fluorescence color changes during the heating process. Thus, the allochroic effect is attributed to the synergistic effect of both heating and photo-inducement (365 nm). Ethanol can turn the heated powder into the initial crystal again which indicates that their thermochromic behavior is reversible and makes the fluorescence recover.

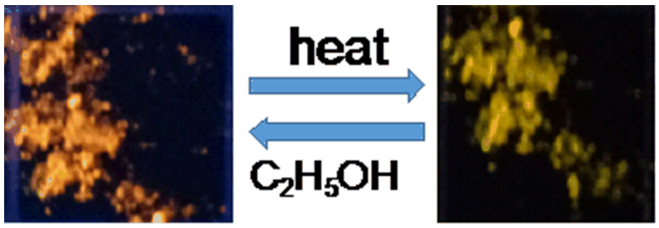

Key words: Thermochromism, Phase transition, Synergistic effect, Photochromism, Fluorescence

I. INTRODUCTION

The thermochromism is a kind of the common stimuli-responsive phenomenon, which is related to the physical or chemical changes of materials caused by the thermal effect. Thermochromic materials change their molecular structure and molecular morphology with temperature [1, 2]. So far, lots of various thermochromic solid materials have been well studied, including inorganic compounds, small-molecule organic compounds, polymers, and metal complexes, *etc.* Although all of them show fascinating thermochromic behaviors, their thermochromisms are different. For inorganic compounds, the changes in the expansion of crystal structures [3] and the size of particles [4] are commonly used to explain the thermochromism. The thermochromism of polymers usually results from the change of intermolecular supramolecular interaction [5]. The mechanisms for the thermochromic metal complexes are various, including changes in ligand conformation [6], binding and dissociating of small molecules [7−10], and charge transfer between central metal ion and ligands [11−15]. There are two kinds of luminous zones as lower-energy band and higher-energy) band in metal complexes [16, 17]. lower-energy band comes from a complex central ion cluster and higher-energy band comes from the ligands, and both of them will change the shape and peak position through regulating temperature [18−20]. Thermochromic organic compounds are usually designed based on the mechanisms of the conversion of enol and ketone structures [21], an open or closed ring of a helical compound [22], structural change in the crystal state [23], and so

*Author to whom correspondence should be addressed. E-mail: xuwq@jlu.edu.cn

on. For crystal state materials, solid thermal discoloration, including the crystal-to-crystal [24] or crystal-to-amorphous transformation [25] is all the reasons for achieving the thermochromic natures. The conversion between different crystal types is reversible. As a result, its thermochromic process is reversible. However, for the conversion between the amorphous and crystal states, mostly, it exhibits an irreversible thermochromism [26].

1,4-Bis[2-(4-pyridyl)ethenyl]-benzene (bpeb) and its derivatives that contain special functional groups like double bond and pyridine have been widely applied in the fields of ion detection [27], coordination compound [28, 29], metal-organic frameworks (MOF), [30] co-crystal materials [31, 32], laser Raman molecular probe [33, 34], and molecular self-assembly [35, 36] *etc.* With the pyridine groups at both ends of bpeb, it is easy to form pyridine salt structure, which is conducive to further modification with alky chains.

In this work, bpeb and its derivatives, DC8, DC12, DC16 (Scheme 1) were synthesized and characterized by ^{1}HNMR and HRMS. We found that they had a remarkable thermochromic nature with reversibility in solid-state, and DC16 also exhibited the photochromic character. Also, the crystal transformation was affected by both light and heat. The relationship between fluorescence and structure was explored.

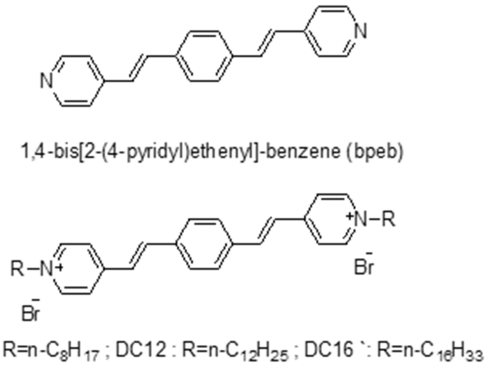

Scheme 1. The molecular structures of bpeb and its derivatives, DC8, DC12, and DC16.

II. EXPERIMENTS

A. Preparation of bpeb, DC8, DC12, DC16

Bpeb is first synthesized according to the report in Ref.[37]. Zinc chloride (13.64 g) was added to 40 mL of acetic anhydride solution containing 13.7 g of 4-methylpyridine and 6.7 g of terephthalaldehyde. The mixture was heated for 8 h under reflux, then cooled to room temperature, and filtered. The precipitates were yellowish powder and they were washed by ethanol and then recrystallized from pyridine. DC8, DC12, and DC16 were synthesized according to Ref.[38]. The synthetic method of DC8 was as follows. Bpeb (2.86 g) and 1-bromooctane (5.79 g, molar ratio of 1:3) were added to 200 mL of DMF. The remaining procedures were the same as those for bpeb. DC12 and DC16 were used through the same procedure as DC8, except that 1-bromooctane was used instead of 1-bromododecane or 1-bromohexadecane, and the molar ratio of bpeb was still 1:3. The coarse products were recrystallized from ethanol. These compounds have been previously reported [39, 40].

B. Instruments

The solid ultraviolet spectrogram was collected by Lambda 950 ultraviolet-visible near-infrared spectrophotometer made by PerkinElmer, and the back base was barium sulfate.

The fluorescent emission spectrum was collected by Ultra-2 micro spectral detection platform, which is a multi-functional, multi-dimensional micro imaging, spectroscopic detection, and micromanipulation system integrating dark field micro imaging, fluorescence micro imaging, laser micro imaging, spectral detection and rapid imaging EMCCD. Samples were put at the heating platform, and the fluorescent emission spectra were collected by a fluorescence spectrophotometer with an excitation light of 365 nm.

C. ^{1}H NMR, ^{13}C NMR, FT-IR, and HRMS measurements

DC8: ^{1}H NMR (500 MHz, DMSO-d_6) δ/ppm 9.01 (d, J=6.5 Hz, 4H, pyridyl), 8.29 (d, J=6.5 Hz, 4H; pyridyl), 8.09 (d, J=16.4 Hz, 2H; vinyl), 7.89 (s, 4H; phenyl), 7.66 (d, J=16.3 Hz, 2H; vinyl), 4.52 (t, J=7.2 Hz, 4H; methylene), 2.03−1.80 (m, 4H; methylene), 1.36−1.17 (m, 20H; methylene), 0.87 (t, J=6.7 Hz, 6H; methyl) (FIG. S1 in supplementary materials). ^{13}C NMR (126 MHz, DMSO) δ/ppm 144.86, 140.26, 137.41, 129.28, 125.04, 124.53, 60.31, 31.60, 31.02, 28.92, 28.83, 25.91, 22.51, 14.41 (FIG. S4 in supplementary materials). HRMS (ESI): m/z calc. for $C_{36}H_{50}N_2{}^{2+}$: 510.3963, $[M/2]^+$; Found: 255.1955 (FIG. S7 in supplementary materials). FT-IR: 3014, 2958, 2927, 2860, 1611, 1507, 1461, 1162 cm^{-1} (FIG. S10(a)

DOI:10.1063/1674-0068/cjcp2008135

in supplementary materials).

DC12: ^{1}H NMR (500 MHz, DMSO-d_6) δ/ppm 9.00 (d, J=6.0 Hz, 4H; pyridyl), 8.28 (d, J=5.9 Hz, 4H; pyridyl), 8.08 (d, J=16.3 Hz, 2H; vinyl), 7.88 (s, 4H; phenyl), 7.65 (d, J=16.3 Hz, 2H; vinyl), 4.52 (t, J=6.5 Hz, 4H; methylene), 1.92 (s, 4H; methylene), 1.27 (d, J=24.3 Hz, 36H; methylene), 0.85 (d, J=6.6 Hz, 6H; methyl) (FIG. S2 in supplementary materials), ^{13}C NMR (126 MHz, DMSO) δ/ppm 144.87, 140.26, 137.42, 129.28, 125.04, 124.53, 60.31, 31.76, 30.99, 29.47, 29.36, 29.23, 29.18, 28.84, 25.88, 22.56, 14.42 (FIG. S5). HRMS (ESI): m/z calc. for $C_{44}H_{66}N_2{}^{2+}$: 622.5215, $[M/2]^+$; Found 311.2588 (FIG. S8 in supplementary materials). FT-IR: 3014, 2958, 2927, 2860, 1611, 1507, 1461, 1162 cm^{-1} (FIG. S10(b) in supplementary materials).

DC16: ^{1}H NMR (500 MHz, DMSO-d_6) δ/ppm 8.99 (d, J=4.8 Hz, 4H; pyridyl), 8.27 (d, J=5.1 Hz, 4H; pyridyl), 8.07 (d, J=16.0 Hz, 2H; vinyl), 7.88 (s, 4H; phenyl), 7.65 (d, J=15.8 Hz, 2H; vinyl), 4.51 (s, 4H; methylene), 1.92 (s, 4H; methylene), 1.23 (s, 52H; methylene), 0.85 (s, 6H; methyl) (FIG. S3 in supplementary materials), ^{13}C NMR (151 MHz, DMSO) δ/ppm 153.06, 144.86, 140.26, 129.28, 129.00, 124.53, 60.33, 31.76, 30.98, 29.51, 29.17, 28.83, 25.86, 22.56 (FIG. S6 in supplementary materials). HRMS (ESI): m/z calc. for $C_{52}H_{82}N_2{}^{2+}$: 734.6467, $[M/2]^+$; Found: 367.3270 (FIG. S9 in supplementary materials). FT-IR: 3014, 2958, 2927, 2860, 1611, 1507, 1461, 1162 cm^{-1} (FIG. S10(c) in supplementary materials).

III. RESULTS AND DISCUSSION

FIG. 1(a) shows solid absorption ultraviolet-visible spectra of bpeb, DC8, DC12, and DC16. Four compounds had the same absorption peak at 229 nm, which is from bpeb. Bpeb has another broad absorption peak at 350 nm. Owing to the linking of an alkyl chain, this band decreases (DC8 and DC12). However, for the alkyl chain containing 16 carbons, a new peak at about 400 nm appears and is stronger than others. The peak at 400 nm is due to the hydrophobic effect. Absorption ultraviolet-visible spectra of DC16 at 1.0×10^{-5} mol/L containing different ratios of water to ethanol were obtained (FIG. 1(b)). DC16 containing ethanol had two absorption peaks at 252 and 382 nm. With the ratio of water increasing, the peak at 382 nm moved to 361 nm, and a new peak at 424 nm appeared. The fluorescence quantum yield measurements (365 nm excitation) showed their fluorescence quantum yields are 2.83%, 4.5%, 5.59% and 4.08% for bpeb, DC8, DC12, and DC16, respectively, indicating that the fluorescence efficiencies of the cationic pyridine DC8, DC12, and DC16 are higher than that of bpeb.

Next, we carried out a thermal gravimetric analysis (TGA) test for the thermogravimetric analysis (FIG. S11−S13 in supplementary materials). DC8 began to lose weight at 250 °C, DC12 at 200 °C, and DC16 at 220 °C, respectively, indicating that the three derivatives had good thermal stability because their thermal decomposition temperatures are all above 200 °C. All three compounds suffered from multiple weight loss and finally lost weight completely at 450 °C, with the final residual mass ratio of about 10%.

FIG. 2 presents the fluorescent spectra of DC8 during the temperature circle. It can be observed that DC8 has one emission band located at 642 nm at room temperature (25 °C). When the temperature increased to 60 °C, the intensity of fluorescence decreased sharply. With the temperature further increasing, the fluorescence intensity decreased ulteriorly, and the fluorescent peak blue-shifted to 544 nm. When the temperature decreased from 120 °C to 25 °C, as shown in FIG. 2(b), the intensity of fluorescence increased and a new emission peak appeared at 544 nm, indicating that the thermochromism is irreversible. Similar phenomena were also observed from the thermochromic processes of DC12 and DC16 under 120 °C (FIG. S14 and S15 in supplementary materials). So we attributed the main thermochromic group to bpeb. ^{1}H NMR spectra of DC8, DC12, DC16 after being heated were obtained (FIG. S18−S20 in supplementary materials). It indicates that the compounds kept the same structure after being heated.

To study the effect of laser light on the samples, we measured the fluorescent spectra of solids at an interval of one minute without heating. As shown in FIG. S16 and S17 (supplementary materials), as time went by, the fluorescence intensity of DC8 and DC12 increased. The change of the intensity was less than 10%, indicating that the laser light source has almost no effect on DC8 and DC12. However, for DC16, it responded to 365 nm light (FIG. 3). At 365 nm light, the peaks at 552 nm and 568 nm both decreased, while the peak at 625 nm increased as well. It exhibited an obvious apparent response to 365 nm light. After 3 min, the intensity of fluorescence stayed unchanged. From FIG. S21

DOI:10.1063/1674-0068/cjcp2008135

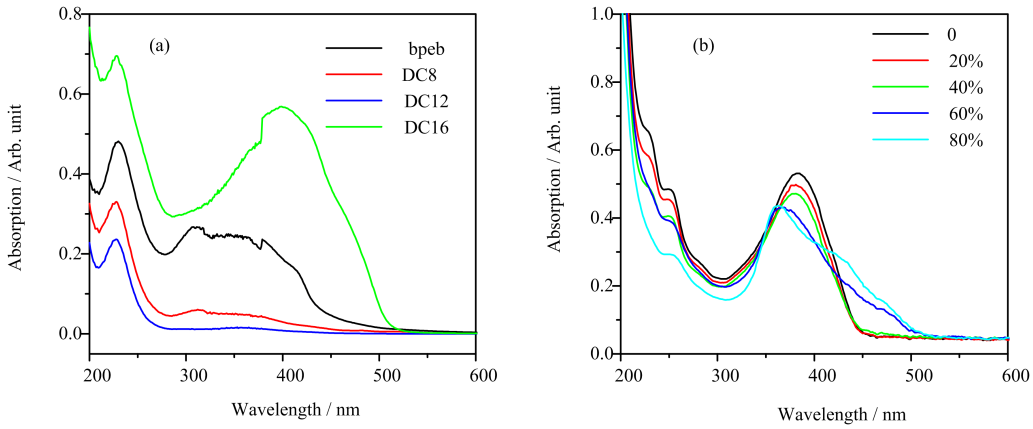

FIG. 1 (a) Solid absorption ultraviolet-visible spectra of bpeb, DC8, DC12, and DC16, respectively. (b) Absorption ultraviolet-visible spectra of DC16 at 1.0×10^{-5} mol/L, water content in ethanol (volume ratio) was 0, 20%, 40%, 60%, and 80%, respectively.

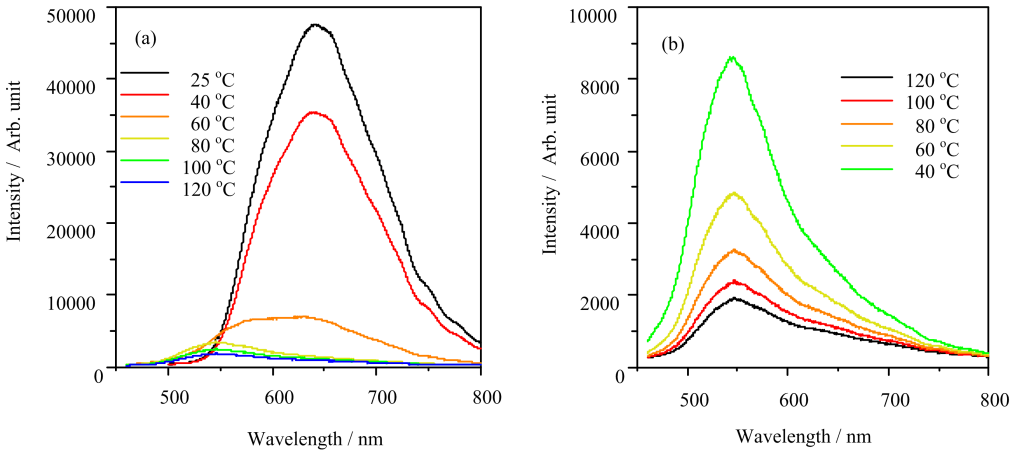

FIG. 2 Fluorescent spectra of DC8 at different temperatures in (a) the temperature-rise period or (b) the temperature-fall period.

in supplementary materials, new peaks appeared after the irradiation of laser light. The new peaks match the structure of C16 that DC16 breaks a chain of carbons. There is an equilibrium between DC16 and C16. C16 seems midbody, and cannot be separated alone. After 6 min, the intensity of the fluorescence of DC8, DC12, and DC16 remained stable.

Powder X-ray diffraction (PXRD) measurements of DC8, DC12, DC16 were carried out to prove the changes in the crystal states before and after heating (FIG. 4). There are apparent diffraction peaks at the PXRD of DC8, DC12, and DC16. Compared with DC8, DC12 and DC16 exhibited stronger diffraction peaks, indicating that they had better crystallization properties with increasing carbon chain length. The diffraction peaks decreased after heating. It indicates that their solid structures have changed from crystal to amorphous state by high temperature. When ethanol was added to the powder, the diffraction peaks recovered. It indicates that their solid structures return to crystal.

Differential scanning calorimetry (DSC) was carried out for DC8, DC12, DC16 solids to explore their phase transition (FIG. S22−S24 in supplementary materials). The DSC test conditions were as follows: the room temperature procedure was up to 130 °C, the heating rate was 10 °C/min, the temperature was maintained for 2 min after the heating, and the temperature returned to 20 °C with the 10 °C/min procedure, and three cycles were repeated. The endothermic peak of DC8 appeared at 93 °C, which indicates that the phase transition occurred. Two endothermic peaks of DC12 appeared at 101 °C and 137 °C, while the endothermic peak of DC16 appeared at 120 °C. With the length of the carbon chain increasing, the temperature of phase

DOI:10.1063/1674-0068/cjcp2008135

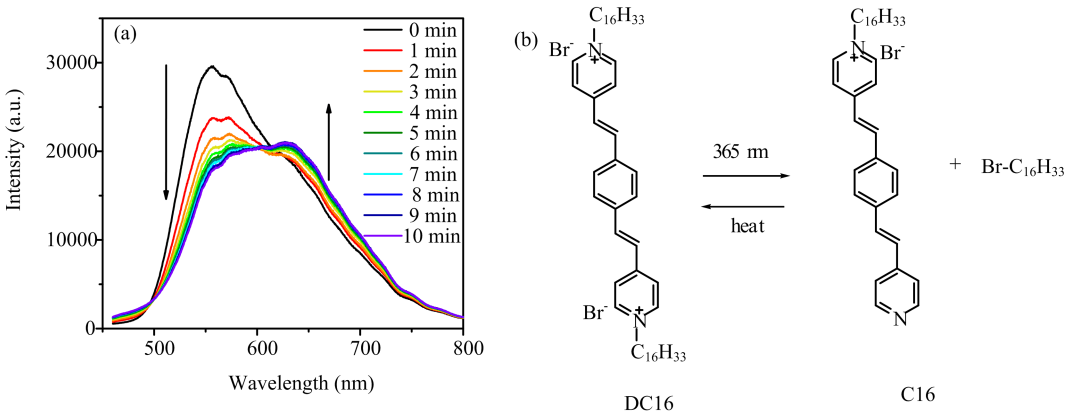

FIG. 3 (a) Fluorescent spectra of DC16 at different time under the excitation wavelength of 365 nm. (b) Mechanism of the fluorescent change of DC16 after the irradiation of laser light.

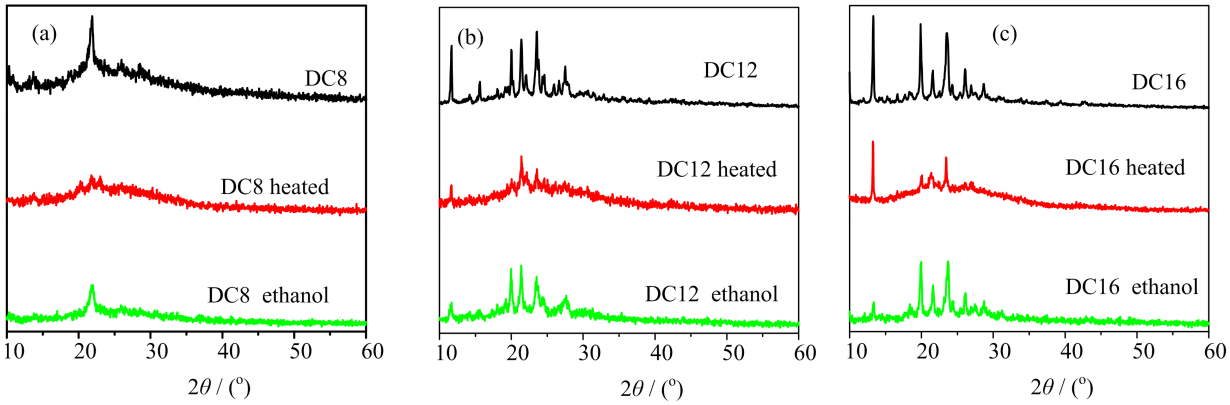

FIG. 4 PXRD of (a) DC8, (b) DC12, (c) DC16 before and after being heated, and exposure to ethanol.

transition increases as well. The peak area of DC8 is less than those of DC12 and DC16, suggesting that the phase transition of DC8 requires less energy, which coincides with the PXRD results. The temperature of the fluorescence was lower than that of phase transition at DSC. It was caused by the 365 nm laser light source, which made the temperature of the phase transition lower than others.

As mentioned above, the thermochromism of DC8, DC12, and DC16 resulting from phase transition from crystal to the amorphous state is irreversible. It is well known that some solvent can transform the powder into the crystal again [25]. After the compound was heated, ethanol was added into the powder. By recrystallizing the solid, we continued the experiments of heating and cooling, and the fluorescent spectra were collected under the excitation of 365 nm (FIG. 5(a)). Similar to FIG. 2, when the temperature changed from 25 °C to 120 °C, the fluorescence change of DC8 has a similar trend. When cooled to 25 °C, the fluorescence peak still kept at 544 nm, and the intensity of fluorescence increased. When ethanol was added to the powder, the fluorescence peak returned to 642 nm. The intensity of fluorescence was a little lower than that of the beginning. It is because the effect of the laser causes the crystal a little disordered. When the sample was heated to 120 °C again, the fluorescent peak moved to 544 nm. The intensity of fluorescence decreased sharply as same as the first time. When the temperature was cooled to 25 °C again, the intensity of fluorescence increased. Via adding ethanol to powder, a reversible fluorescence cycle was realized. Similar phenomena were observed at the fluorescence emission spectra of DC12 and DC16 (FIG. 5 (b) and (c)). However, the fluorescent emission spectra of DC16 were a little different when ethanol was added. The fluorescence did not return to the original one of 25 °C, and it was similar to that in FIG. 3 (a), which can be explained by the photochromic character of DC16 as discussed above.

DOI:10.1063/1674-0068/cjcp2008135

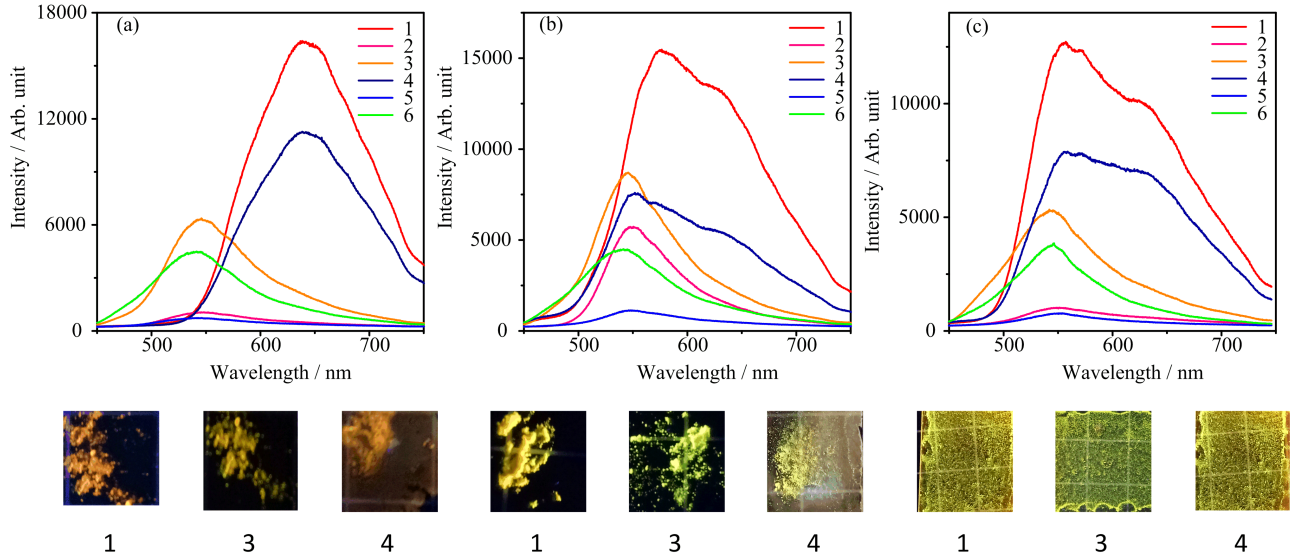

FIG. 5 Fluorescent spectra of (a) DC8, (b) DC12, (c) DC16 under different conditions: (1) 25 °C, (2) heated to 120 °C, (3) cooled to 25 °C, (4) ethanol was added for the compound at 25 °C, (5) heated to 120 °C again, (6) cooled to 25 °C. Photographs of processes 1, 3, 4 are also given.

IV. CONCLUSION

In summary, bpeb and its derivatives were synthesized and they exhibited thermochromic feature, which is evidenced to be the phase transition from crystalline to amorphous states via DSC and PXRD. With the increase of the alkyl chain length, DC12 and DC16 showed better crystallinity. The 365 nm light made chemical bond rotate, which played a synergistic role in making the phase-transition temperature lower. Ethanol has been proven to recrystallize the powders to crystals and recover their fluorescence. Thus, the circle of the fluorescence can be achieved by heating, cooling and ethanol solvent recrystallization via the flexible transition between crystalline and amorphous states. DC8, DC12, DC16 had excellent thermochromic properties and potential applications at the heat-sensing technique. This study is of significance for understanding the structure-property relation and guides thermochromic molecular design.

Supplementary materials: ^{1}H NMR spectra, ^{13}C NMR spectra, mass spectra, FT-IR, TGA, fluorescent spectra, and DSC of DC8, DC12, DC16 are available.

V. ACKNOWLEDGMENTS

This work was supported by the National Natural Science Foundation of China (No.21573092, No.21573087 and No.21873039)

[1] E. Hadjoudis, and I. M. Mavridis, Chem. Soc. Rev. **33**, 579 (2004).
[2] O. S. Wenger, Chem. Rev. **113**, 368 (2013).
[3] S. Kumar, A. Qadir, F. Maury, and N. Bahlawane, ACS Appl. Mater. Inter. **9**, 21447 (2017).
[4] Y. Ge, Z. H. Shah, C. Wang, J. Wang, W. Mao, S. Zhang, and R. Lu, ACS Appl. Mater. Inter. **7**, 26437 (2015).
[5] H. Kim, and J. Y. Chang, Langmuir **30**, 13673 (2014).
[6] M. Dosen, Y. Kawada, S. Shibata, K. Tsuge, Y. Sasaki, A. Kobayashi, M. Kato, S. Ishizaka, and N. Kitamura, Inorg. Chem. **58**, 8419 (2019).
[7] T. Gong, X. Yang, J. J. Fang, Q. Sui, F. G. Xi, and E. Q. Gao, ACS Appl. Mater. Inter. **9**, 5503 (2017).
[8] P. K. Tsobnang, J. L. Ngolui, E. Wenger, P. Durand, S. Dahaoui, and C. Lecomte, Cryst. Growth Des. **17**, 4908 (2017).
[9] P. Hao, C. Guo, M. Wang, J. Shen, and Y. Fu, Inorg. Chem. **58**, 3364 (2019).
[10] G. Shin, M. I. Khazi, and J. M. Kim, Macromolecules **53**, 149 (2019).
[11] L. Tom and M. R. P. Kurup, Dalton T, **48**, 16604 (2019).
[12] D. A. Turchetti, R. A. Domingues, C. Zanlorenzi, B. Nowacki, T. D. Z. Atvars, and L. C. Akcelrud, J. Phys. Chem. C **118**, 30079 (2014).
[13] D. A. Turchetti, A. J. Santana, L. G. T. A. Duarte, T. D. Z. Atvars, R. A. Domingues, and L. Akcelrud, Polymer **177**, 65 (2019).

DOI:10.1063/1674-0068/cjcp2008135

[14] R. Wei, P. Song, and A. Tong, J. Phys. Chem. C **117**, 3467 (2013).
[15] T. Yu, L. An, L. Zhang, J. Shen, Y. Fu, and Y. Fu, Cryst. Growth. Des. **14**, 3875 (2014).
[16] Y. He, Y. R. Huang, Y. L. Li, H. H. Li, Z. R. Chen, and R. Jiang, Inorg. Chem. **58**, 13862 (2019).
[17] F. Parmeggiani and A. Sacchetti, J. Chem. Educ. **89**, 946 (2012).
[18] X. C. Shan, H. B. Zhang, L. Chen, M. Y. Wu, F. L. Jiang, and M. C. Hong, Cryst. Growth Des. **13**, 1377 (2013).
[19] L. Wang, Y. Ye, Z. Li, Q. Lin, J. Ouyang, L. Liu, Z. Zhang, and S. Xiang, Cryst. Growth Des. **17**, 2081 (2017).
[20] K. Yang, S. L. Li, F. Q. Zhang, and X. M. Zhang, Inorg. Chem. **55**, 7323 (2016).
[21] M. Hu, F. Xing, Y. Zhao, Y.L. Bai, M. X. Li, and S. Zhu, ACS Omega **2**, 1128 (2017).
[22] B. Mondal, A. K. Ghosh, and P. S. Mukherjee, J. Org. Chem, **82**, 7783 (2017).
[23] M. Ibarra-Rodri Guez, B. M. Munoz-Flores, H. V. Dias, M. Sanchez, A. Gomez-Trevino, R. Santillan, N. Farfan, and V. M. Jimenez-Perez, J. Org. Chem. **82**, 2375 (2017).
[24] S. Ito, C. Nishimoto, and S. Nagai, CrystEngComm **21**, 5699 (2019).
[25] F. Xu, T. Nishida, K. Shinohara, L. Peng, M. Takezaki, T. Kamada, H. Akashi, H. Nakamura, K. Sugiyama, K. Ohta, A. Orita, and J. Otera, Organometallics **36**, 556 (2017).
[26] W. Jeong, M. I. Khazi, D. G. Lee, and J. M. Kim, Macromolecules **51**, 10312 (2018).
[27] Y. Yang, X.L. Ni, T. Sun, H. Cong, and G. Wei, RSC Adv. **4**, 47000 (2014).
[28] V. W. W. Yam, V. C. Y. Lau, and L. X. Wu, J. Chem. Soc. Dalton 1461 (1998).
[29] B. J. Coe, J. L. Harries, J. A. Harris, B. S. Brunschwig, P. N. Horton, and M. B. Hursthouse, Inorg. Chem. **45**, 11019 (2006).
[30] I. H. Park, C. E. Mulijanto, H. H. Lee, Y. Kang, E. Lee, A. Chanthapally, S. S. Lee, and J. J. Vittal, Cryst. Growth Des. **16**, 2504 (2016).
[31] B. R. Bhogala, and A. Nangia, Cryst. Growth Des. **3**, 547 (2003).
[32] M. Khan, V. Enkelmann, and G. Brunklaus, Cryst. Growth Des. **9**, 2354 (2009).
[33] J. Cheng, X. Li, W. Song, W. Xu, B. Zhao, and G. Zhang, Chem. Phys. Lett. **405**, 344 (2005).
[34] H. Jia, W. Xu, J. An, D. Li, and B. Zhao, Spectrochim. Acta Part A **64**, 956 (2006).
[35] R. Balgley, G. de Ruiter, G. Evmenenko, T. Bendikov, M. Lahav, and M. E. van der Boom, J. Am. Chem. Soc. **138**, 16398 (2016).
[36] X. L. Ni, S. Chen, Y. Yang, and Z. Tao, J. Am. Chem. Soc. **138**, 6177 (2016).
[37] A. V. Gutov, E. B. Rusanov, L. V. Chepeleva, S. G. Garasevich, A. B. Ryabitskii, and A. N. Chernega, Russ. J. Gen. Chem. **79**, 1513 (2009).
[38] Y. Yang, S. Chen, and X. L. Ni, Anal. Chem. **87**, 7461 (2015).
[39] E. Stathatos, P. Lianos, R. H. Rakotoaly, A. Laschewsky, and R. Zana, J. Colloid. Interf. Sci. **227**, 476 (2000).
[40] S. K. Samanta and S. Bhattacharya, J. Mater. Chem. **22**, 25277 (2012).

DOI:10.1063/1674-0068/cjcp2008135